Journal of Machine Engineering, 2025, Vol. 25
ISSN 1895-7595 (Print) ISSN 2391-8071 (Online)

Received*: 07 February 2025* / Accepted: *22 April 2025* / Published online: *23 May*

simulation,
biofuel,
emissions,
reactive flow

Aliya ASKAROVA[1], Saltanat BOLEGENOVA[1],
Shynar OSPANOVA[1*], Karlygash BOLEGENOVA[1],
Alfiya NURMUKHANOVA[1]

SIMULATION OF THE EFFECTIVE DISTRIBUTION OF BIOFUEL DROPLETS IN A REACTING FLOW

This work is devoted to developing a universal model of atomization and combustion of biofuel droplets using a statistical approach and a particle trajectory tracking model. The model applies to all types of biodiesel used in internal combustion engines with direct injections and is designed to optimize combustion processes, reduce emissions, and improve engine efficiency. Based on mathematical equations of conservation of mass, momentum, and energy, as well as numerical methods for calculating complex turbulent flows and the droplet atomization process, complex computational experiments were carried out using modern technologies. Research has shown that biodiesel has higher combustion temperatures and better evaporation characteristics compared to diesel fuel, which helps to reduce carbon oxides and soot emissions. The results of modelling the effect of pressure in the combustion chamber on the combustion process showed that its increase reduces soot emissions and promotes more complete fuel combustion. Visualization of aerodynamic and temperature profiles confirms the high efficiency of biodiesel combustion, especially under high temperature and pressure conditions.

1. INTRODUCTION

The global biofuel market is rapidly developing due to environmental issues and the rising prices of oil and gas. According to the International Energy Agency (IEA), global biofuel production has increased by 25% by 2024, reaching 76.3 million tons, which is 7% more compared to the previous year. The United States, Brazil, and Indonesia significantly expanded biodiesel production, accounting for nearly 60% of the global volume. In the United States, biodiesel production nearly doubled, reaching around 21 million tons (Fig. 1) [1, 2].

Kazakhstan has a state policy on bioenergy, which promotes biotechnology integration into the economy. The biodiesel combustion in Kazakhstan offers both environmental and economic advantages. The country's raw materials have significant potential, enabling it to

[1] Department of Thermal Physics and Technical Physics, Al-Farabi Kazakh National University, Kazakhstan
[*] E-mail: s.osspanova@gmail.com
https://doi.org/ 10.36897/jme/204226

become one of the world's largest biofuel producers, following Brazil, the USA, and China. Kazakhstan is home to two biodiesel and bioethanol production plants that use advanced wheat processing technologies with minimal waste and the production of bio-additives. The products are exported to Russia, Uzbekistan, Europe, and China.

Biodiesel is an important alternative to hydrocarbon fuels, contributing to the reduction of CO2 emissions and improving air quality. However, its combustion may release nitrogen oxides and carbon monoxide [3–5]. To fully harness the potential of biodiesel, it is crucial to apply modern simulation techniques that optimize combustion, reduce emissions, and enhance engine efficiency, thereby lowering fuel consumption and pollution.

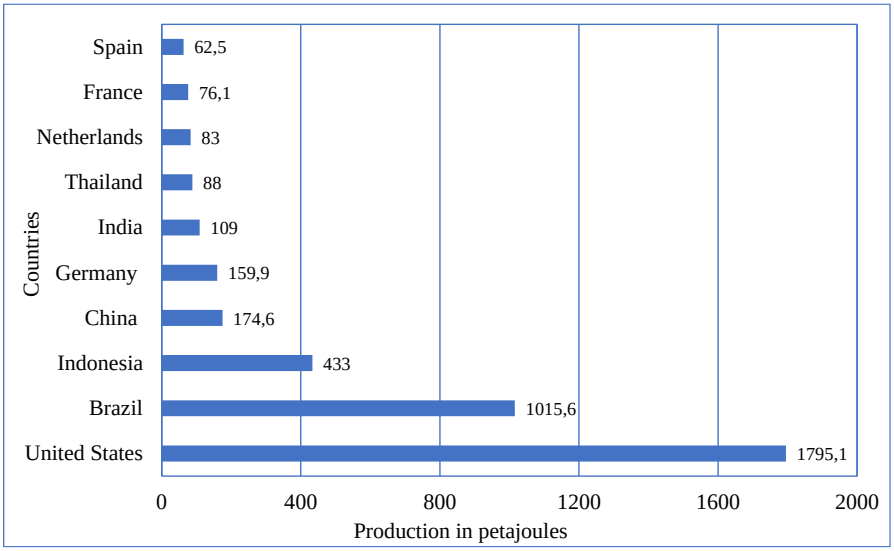

Fig. 1. Leading countries based on biofuel production worldwide in 2024

The combustion characteristics, performance, and emissions when using different biodiesels in compression ignition engines were investigated in [6]. The works [7, 8] present predictive models of biodiesel properties aimed at improving their accuracy, as well as an evaluation of these properties to optimize engine performance. A multi-stage combustion model for biodiesel engines, which allows for more accurate prediction of combustion processes and helps optimize engine performance, was proposed by the authors in [9]. In [10], a simplified soot model for the combustion of diesel and biodiesel was suggested, which contributes to a more accurate prediction of soot particle formation and reduction of emissions. The combustion characteristics, emissions, and engine performance when using blends of rapeseed biodiesel with diesel fuel were investigated in [11].

In [12] the use of biodiesel produced from non-edible rapeseed oil via transesterification as an alternative fuel for diesel engines was investigated. Experiments were conducted on a 5.95 kW single-cylinder direct injection diesel engine, using diesel, biodiesel, and diesel-biodiesel blends at 200 bar injection pressure. Key parameters such as thermal efficiency, specific energy consumption, exhaust gas temperature, in-cylinder pressure, heat release, ignition delay, and emissions (HC, CO, NOx, and soot) were analyzed. The results showed that the B25 blend (25% biodiesel, 75% diesel) can be used without engine modifications, offering good thermal efficiency and reduced emissions.

Research shows that rapeseed biodiesel (both pure and blended with diesel) has lower thermal efficiency and higher specific fuel consumption. However, CO and particulate emissions are reduced by 60%, while CO2 and NOx emissions increase. This is due to the reduced ignition delay and advanced fuel injection when using rapeseed biodiesel [13].

However, the main drawbacks of all these studies are the simplification of the models, their limited applicability to other types of liquid fuels, and the lack of thorough validation of the results.

This work aims to develop a universal model for the atomization and combustion of biodiesel droplets using a statistical approach and a particle tracking model, followed by the validation of the numerical results. The model applies to all types of biodiesel used in direct injection (DI) internal combustion engines.

In Europe, the most popular feedstock for biofuel production is rapeseed oil, which accounted for more than 50% of the total in 2024, according to the International Institute for Sustainable Development. In Kazakhstan, where enterprises producing key components for biodiesel such as soybeans and rapeseed oil are actively developing, the biofuel used in this study was biodiesel RME B100. This is a pure biodiesel consisting of 100% rapeseed methyl ester, without the addition of traditional diesel fuel.

2. A COMPREHENSIVE MODEL OF THE PROBLEM

The mathematical model of atomization and combustion of liquid fuel droplets is based on the conservation equations of mass, momentum, internal energy, and reactant concentration in a two-phase flow.

2.1. THE GOVERNING EQUATIONS OF SPRAY DYNAMICS IN TWO-PHASE REACTING FLOW

The mass conservation equation for a two-phase flow is as follows [14]:

$$\frac{\partial \rho}{\partial t} + div(\rho \boldsymbol{u}) = S_{mass}, \tag{1}$$

where u is the velocity of the liquid fuel flow, and S_{mass} is the source term arising due to changes in the gas density during evaporation.

The momentum conservation equation for a two-phase flow is as follows [14]:

$$\rho \frac{\partial u}{\partial t} + \rho(grad\boldsymbol{u})\boldsymbol{u} = div\boldsymbol{\xi} + \rho \boldsymbol{g} + S_{mom}, \tag{2}$$

where S_{mom} is the source term representing the local rate of momentum change in the gas phase due to the motion of the droplets.

The equation for the conservation of internal energy is as follows [14]:

$$\rho \frac{\partial E}{\partial t} = \boldsymbol{\tau}: \boldsymbol{D} - \rho div\boldsymbol{u} - div\boldsymbol{q} + S_{energy}, \tag{3}$$

where q is the heat flux, expressed by Fourier's law, and S_{energy} is the source term due to the contribution of the internal energy change caused by the fuel droplet motion.

The equation for the conservation of the concentration of component m is as follows [15]:

$$\frac{\partial(\rho c_m)}{\partial t} = -\frac{\partial(\rho c_m u_i)}{\partial x_i} + \frac{\partial}{\partial x_i}\left(\rho D_{c_m}\frac{\partial c_m}{\partial x_i}\right) + S_{mass}, \tag{4}$$

where ρ_m is the mass density of component m, and ρ is the total mass density.

The turbulent characteristics of the reacting flow are calculated using a two-parameter empirical k-ε turbulence model, which includes the equations for turbulent kinetic energy k and its dissipation rate ε [16, 17]:

$$\rho\frac{\partial k}{\partial t} + \rho\frac{\partial \bar{u}_j k}{\partial x_j} = \frac{\partial}{\partial x_j}\left[\left(\mu + \frac{\mu_t}{\sigma_k}\right)\frac{\partial k}{\partial x_j}\right]\frac{\partial \bar{u}_i}{\partial x_j} + G - \frac{2}{3}\rho k\delta_{ij}\frac{\partial \bar{u}_i}{\partial x_j} - \rho\varepsilon, \tag{5}$$

$$\rho\frac{\partial \varepsilon}{\partial t} + \rho\frac{\partial \bar{u}_j \varepsilon}{\partial x_j} - \frac{\partial}{\partial x_j}\left[\left(\mu + \frac{\mu_t}{\sigma_\varepsilon}\right)\frac{\partial \varepsilon}{\partial x_j}\right] = c_{\varepsilon_1}\frac{\varepsilon}{k}G - \left[\left(\frac{2}{3}c_{\varepsilon_2} - c_{\varepsilon_3}\right)\rho\varepsilon\delta_{ij}\frac{\partial \bar{u}_i}{\partial x_j}\right] - c_{\varepsilon_2}\rho\frac{\varepsilon^2}{k}. \tag{6}$$

The constant values c_{ε_1}, c_{ε_2}, c_{ε_3}, σ_k, σ_ε, which are parameters of the computational model, are typically determined experimentally.

2.2. STATISTICAL MODEL OF ATOMIZATION AND DROPLET DISTRIBUTION IN A REACTING FLOW

This paper is the first to jointly apply a statistical approach and a particle tracking model to study biofuel droplets, which is a novel approach that is usually used separately to model the atomization of traditional liquid fuels.

The distribution and breakup of fuel particles are described using a statistical approach with the Rosin-Rammler distribution [18], which effectively models a wide range of particle sizes, where smaller droplets dominate, but larger ones are also present, as is typical in atomization processes [19]:

$$d_{p_0} + d_p(-ln(1 - n_{rand}k_R))^{-q}, \tag{7}$$

where k_R is defines as $k_R = 1 - exp\left(\frac{\left(d_{p_{max}} - d_{p_0}\right)^q}{\langle d_p\rangle}\right)$, n_{rad} is the random number, d_{p_0} is the minimum diameter, $d_{p_{max}}$ is the maximum diameter, and $\langle d_p\rangle$ is the mean diameter of the droplets. The spread factor of the distribution is controlled by q.

During droplet injection, the main factors contributing to breakup are the densities of the liquid and gas, their relative velocity, the liquid's viscosity, and surface tension [19]. The Weber number, which represents the ratio of liquid inertia to surface tension, is a key dimensionless number for droplet breakup [21]:

$$\mathrm{We_p} = \frac{\rho_g\left|\mathbf{u}_g - \mathbf{u}_p\right|^2 r_p}{\sigma_p}, \tag{8}$$

where ρ_g is gas density, σ_p is the surface tension of the droplet.

Droplets can break up through various modes, depending on velocity, surrounding pressure, and surface tension [22]. These modes include vibrational breakup, bag breakup, streamer breakup, stripping breakup, and catastrophic breakup.

In the present work, the maximum Weber number does not exceed 85. So, the bag breakup model was chosen to describe the secondary breakup of a droplet when it is subjected to shear forces or aerodynamic forces. The droplet forms a "bag" structure, where the droplet deforms and stretches, leading to the formation of a thin film around the edges. Eventually, this film can rupture, causing the droplet to break up into smaller fragments. This is particularly observed when a droplet is in a high-speed environment or subjected to high shear stress.

This work used a particle trajectory tracking model [23], designed to predict the movement of droplets, their behaviour, and interactions with the surrounding environment. The model is implemented using a Lagrangian approach, where each particle is tracked individually and describes its motion over time.

2.3. SPATIAL MODEL OF THE FUEL COMBUSTION

This study used a diesel engine prototype with equal cylinder diameter and piston stroke, ensuring a 1:1 ratio. Figure 2a shows a schematic of the internal combustion engine with design parameters: cylinder bore (D) of 200 mm, piston stroke (S) of 221 mm, nominal speed of 1700 rpm, and a minimum compression ratio of 14 [24]. The engine operates on a four-stroke cycle with a direct injection mechanism, an in-line design, and a liquid cooling system. The injection temperature in the combustion chamber ranged from 800 to 1500 K, while the pressure varied between 20 and 60 bar. Usually four-stroke diesels have one injector only [25].

A cylindrical combustion chamber model was developed, based on the spray mechanism and geometric characteristics of a DI engine. The chamber has a height (Z or H) of 15 cm and a diameter of 4 cm. A general view of the combustion chamber is presented in Fig. 2b. Liquid fuel is injected directly into the chamber through a nozzle located at its lower part.

This study utilizes a multi-reaction chemical kinetics framework, coupled with the CHEMKIN code, to model chemically reactive fuel spray flows in internal combustion engines. This methodology enables a detailed analysis of combustion dynamics and provides the capability to predict the influence of these processes on pollutant emissions, thereby contributing to the development of more efficient and environmentally sustainable engine designs [26].

The modelling was based on experimental data and a predictive correlation that estimates ignition delay time under various engine operating conditions. This approach can be used to analyse and optimize the performance of diesel engines running on biodiesel [27].

The system of equations describes the material balance of chemical reactions are resolved:

$$\frac{\mathrm{d}C_j}{\mathrm{d}\tau} = \sum_j W_{ij}, \tag{9}$$

where C_j is a mole fraction of species j, τ is a time, and W_{ij} is the reaction rate for i reaction and j species.

The global Shell model of soot formation [28] was utilized to predict soot formation during the combustion of hydrocarbon fuels. The model incorporates the processes of nucleation, particle growth, and agglomeration, alongside the pyrolysis of hydrocarbons and the formation of polycyclic aromatic hydrocarbons, which are pivotal in soot formation [29]. This model facilitates the prediction of soot emissions and the optimization of combustion processes, thereby enhancing engine efficiency and mitigating environmental emissions.

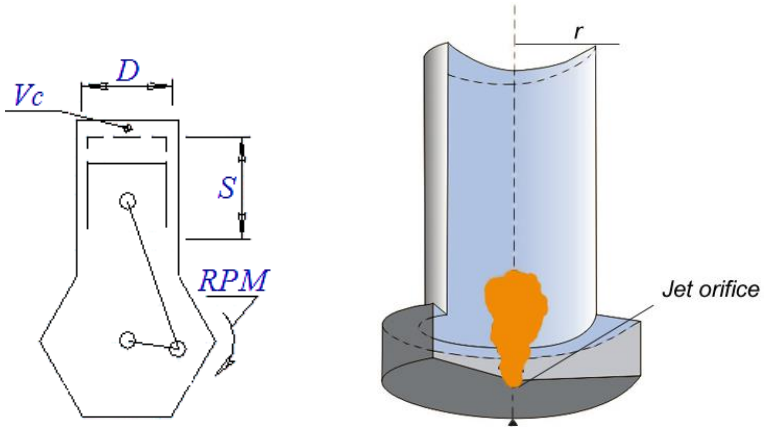

Fig. 2. a) Schematic diagram of a DI internal combustion engine: *D* is cylinder bore, *S* is piston stroke, and V_c is nominal engine speed; b) General view of the combustion chamber

3. RESULTS OF COMPUTATIONAL EXPERIMENTS

3.1. COMPARATIVE ANALYSIS

This paper presents the results of computational modelling of biodiesel and diesel fuel's atomization, combustion, and evaporation processes, which optimizes parameters to reduce carbon oxides and soot emissions from internal combustion engines.

Figure 4 shows a comparative analysis of the combustion temperatures of the reacting mixtures of biodiesel and petroleum diesel, obtained through computational experiments using the developed computer model. The reacting mixture consists of biodiesel or diesel fuel mixed with an oxidizer. Biodiesel is composed entirely of rapeseed methyl ester, while conventional diesel fuel predominantly consists of tetradecane, which is commonly found in the heavier fractions derived from petroleum.

The computer simulations revealed that at a distance of 30 mm from the injector nozzle, the temperature of the biodiesel fuel-air mixture increases from 1900 K to 2700 K, whereas for diesel fuel, the maximum temperature reaches 1800 K (Fig. 4).

During the study of biodiesel's atomization and combustion processes, the Sauter mean diameters of its droplets were measured as a function of the injection temperature (Fig. 5). A comparative analysis was also conducted with the combustion of ethanol, which, like biodiesel, contributes to reducing harmful emissions, improving fuel economy, and reducing dependence on fossil resources.

As the injection temperature increases from 1300 K to 1500 K, the minimum droplet size of biodiesel is 40 to 35 μm, while ethanol droplets range in size from 23 to 20 μm (Fig. 5). Despite the smaller droplet size of ethanol during atomization, its widespread use must take into account its low calorific value, corrosive activity, and the need for modifications to certain engine components.

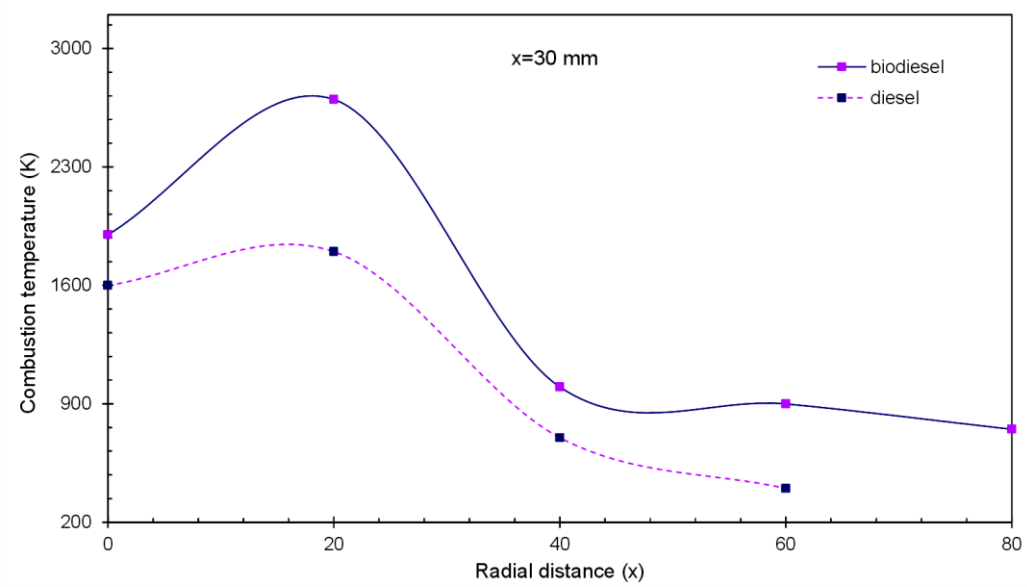

Fig. 4. The combustion temperatures of biodiesel and diesel fuel at a distance of x = 30 mm from the injector

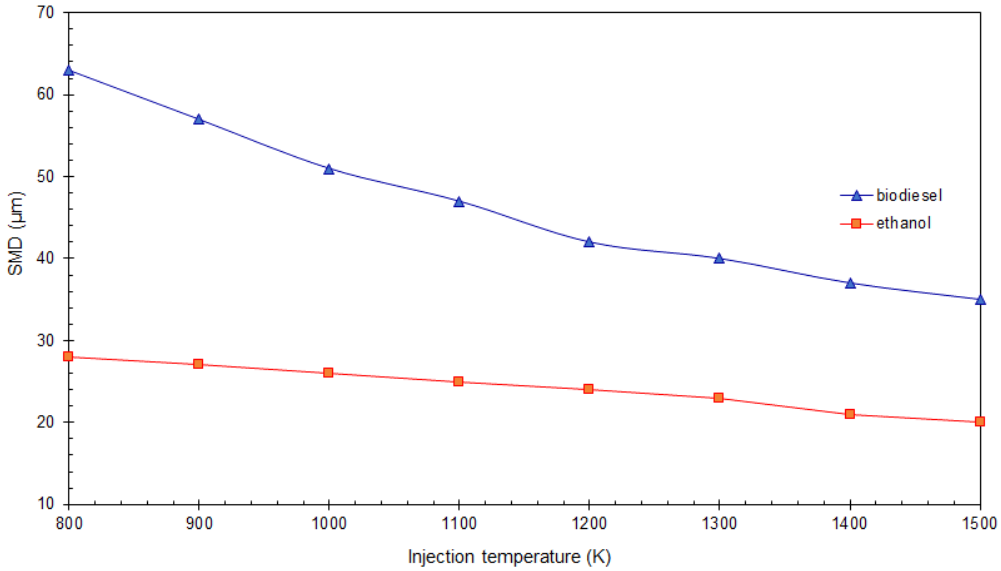

Fig. 5. Sauter mean diameters (SMD) of biodiesel and ethanol droplets as a function of injection temperature

As the injection temperature increases, the droplet diameters of both fuels decrease, as high temperatures promote more intense evaporation of the liquid on the droplet surface and improve its atomization. As a result, the droplets become smaller, which increases their surface area, accelerates the evaporation process, and enhances combustion efficiency.

In this paper, we focused on carbon oxides due to their significantly stronger impact on the greenhouse effect compared to nitrogen oxides (NOx). Although carbon oxides (CO) have a lower ability to directly absorb infrared radiation, their indirect effect through interactions with ozone and methane further intensifies the greenhouse effect. While nitrogen oxides do influence atmospheric processes, their contribution to climate change is comparatively less significant. Thus, the emphasis on carbon oxides is based on their more pronounced role in global warming.

A comparative analysis of the carbon monoxide (CO) concentration distribution during the combustion of biodiesel and diesel fuel as a function of injection temperature is presented in Fig. 6. At temperatures of 800–900 K, the CO emission peak is 2–4 g/g for diesel fuel and 1–2 g/g for biodiesel. As the injection temperature increases, CO emissions decrease, reaching a minimum level of 0.14 g/g during the biodiesel combustion.

At temperatures above 2000 K, the role of plasma processes such as hydrocarbon dissociation and chemical reactions involving ions, as well as excitation of different degrees of freedom of atoms and molecules, increases. However, in this work, it is assumed that combustion processes occur in temperature ranges where CO_2 dissociation does not significantly affect the results. Therefore, a standard model of carbon monoxide concentration distribution was used without taking this effect into account. The focus was on traditional chemical reactions such as carbon and hydrocarbon oxidation. Including thermal dissociation of CO_2 would require more complex chemical kinetics and calculations, which is beyond the scope of the current study. In addition, experimental studies have shown that at high temperatures in the combustion chamber, the degree of carbon oxidation increases, which helps reduce the formation of carbon monoxide. Biodiesel, due to the high oxygen content in the molecules, helps to more effectively oxidize carbon into carbon dioxide (CO_2), which leads to a decrease in the formation of CO [30].

Pressure has a significant impact on soot emissions during the combustion of biodiesel (Fig. 7). Generally, as the pressure in the engine cylinder increases, the combustion process improves, leading to a reduction in soot emissions. This is because higher pressure increases the temperature and compressibility of the mixture, which promotes more complete fuel combustion.

The study found that biodiesel has higher combustion temperatures than diesel fuel, which is attributed to its higher calorific value. As the injection temperature increases, the droplet diameter decreases, improving evaporation and combustion efficiency for both fuels. Regarding emissions, biodiesel combustion results in lower carbon monoxide (CO) levels compared to diesel fuel, especially with increased injection temperature. The pressure in the cylinder also plays a crucial role in reducing soot emissions by enhancing the combustion process and ensuring more complete fuel combustion.

The study found that biodiesel has higher combustion temperatures than diesel fuel, which is attributed to its higher calorific value. As the injection temperature increases, the droplet diameter decreases, improving evaporation and combustion efficiency for both fuels. Regarding emissions, biodiesel combustion results in lower carbon monoxide (CO) levels compared to diesel fuel, especially with increased injection temperature. The pressure in the cylinder also plays a crucial role in reducing soot emissions by enhancing the combustion process and ensuring more complete fuel combustion.

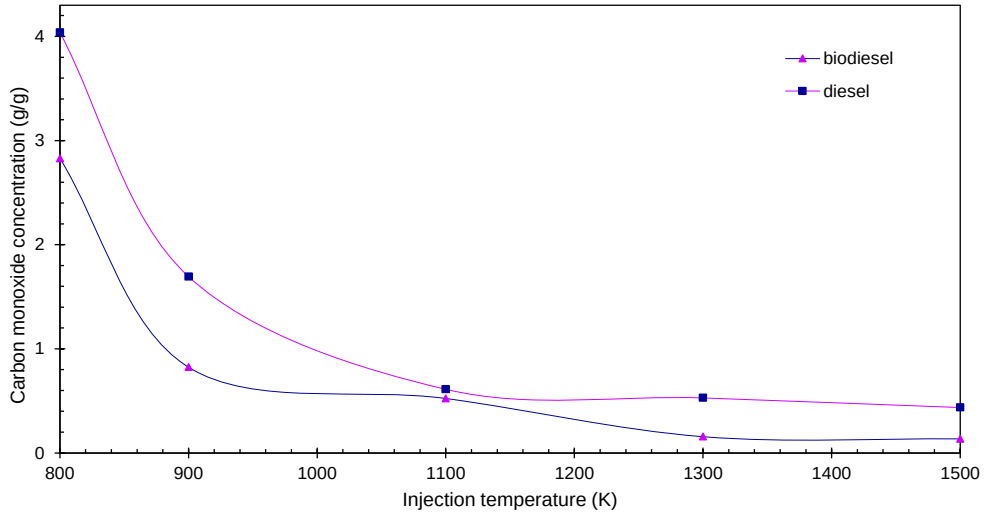

Fig. 6. Distribution of carbon monoxide (CO) concentration during the combustion of biodiesel and diesel fuel

In the future, we plan to conduct simulations of pressure changes over time during the combustion process for both biodiesel and conventional diesel fuel. It is expected that the use of biodiesel will lead to a faster pressure increase due to its higher flammability and more complete combustion. This, in turn, may cause the peak pressure to be reached at an earlier stage. We intend to further study and optimize this process to improve the efficiency and reliability of diesel engines.

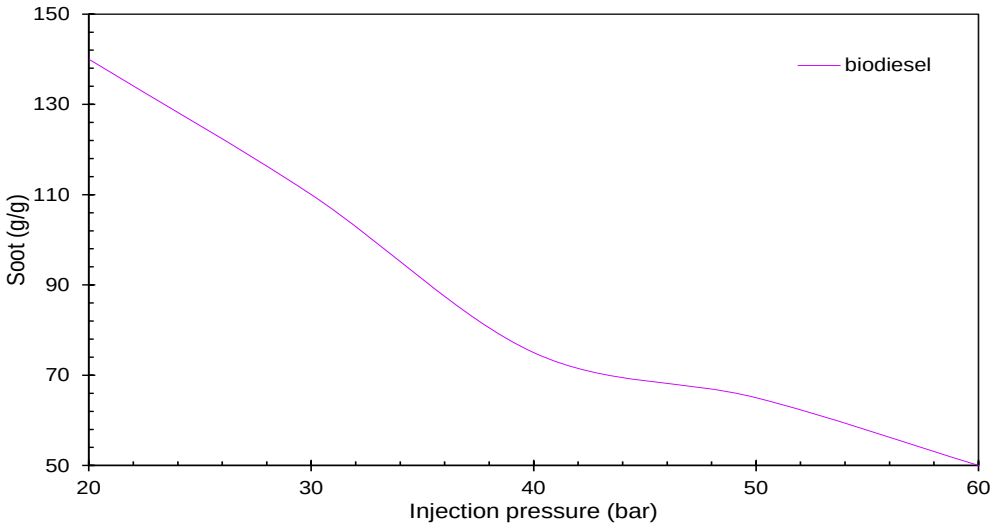

Fig. 7. Soot emissions as a function of injection pressure during the combustion of biodiesel

3.1. 3D VISUALIZATION OF A REACTING FLOW

The following figures (8–12) show the results of 3D visualization of biodiesel fuel's temperature, concentration, and velocity profiles 2.5 ms and 3 ms after the injection, obtained using the developed comprehensive computer model.

Figure 8 shows the temperature profiles of biodiesel at 2.5 ms and 3 ms. At time 2.5 ms after the injection starts, the temperature plume extends from 0.8 cm to 2.4 cm in height and 0.5 cm in width, with temperatures in the plume zone reaching 2490–2700 K (Fig. 8a). 3 ms after the start of injection, the lower part of the temperature plume narrows and moves to the upper part of the combustion chamber, reaching 3 cm (Fig. 8b). This is due to the high heat value, chemical composition, and good oxidizability of biodiesel, which contribute to its more complete and intense combustion compared to diesel fuel.

In previous studies [31] using diesel and gasoline, the maximum combustion temperature in the plume core for both fuels ranged from 1496 to 1802 K depending on the initial injection temperature. These results once again confirm the high efficiency of biodiesel due to its enhanced combustion characteristics.

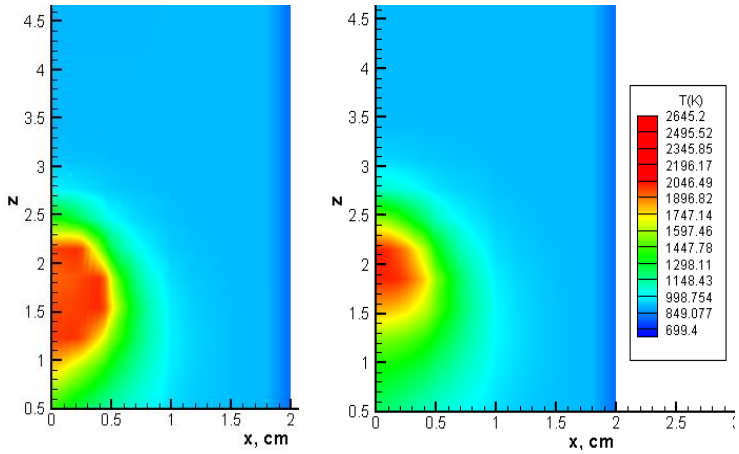

a) 2.5 ms b) 3 ms

Fig. 8. Temperature profiles during biodiesel combustion at a) t = 2.5 ms and b) t = 3 ms after the start of injection: Z (cm) – chamber's height projection; X (cm) – chamber's longitudinal projection

Figure 9 shows the concentration fields of carbon dioxide during the combustion of biodiesel. The high CO_2 concentration (0.06 g/g) along the axis of the combustion chamber is due to more complete combustion and higher oxygen consumption, indicating a greater oxidizability of biodiesel compared to diesel fuel.

When gasoline and traditional diesel fuel are burned, CO_2 emissions range from 0.08 to 0.12 g/g. Increasing the diesel fuel injection rate slightly reduces CO_2 emissions due to incomplete combustion, as the fuel droplets do not fully oxidize within the combustion chamber [14]. Studies [15] of the injection angle effect have shown that with an increase in the injection angle from 4 to 10 degrees, the concentration of CO_2 formed during combustion of diesel fuel increases from 0.180 g/g to 0.182 g/g. At the same time, during combustion of gasoline, the opposite trend is observed: with an increase in the injection angle, the amount of CO_2 released decreases, reaching a value of 0.176 g/g at angles of 6-8 degrees.

Figure 10 shows the dispersion of biodiesel droplets by size at 2.5 ms and 3 ms. The droplet distribution follows the Rosin-Rammler function, which we applied in the statistical approach. In the lower part of the combustion chamber, where droplets with sizes ranging from 40 to 65 μm dominate, the distribution exhibits a characteristic high value of the parameter q, indicating the predominance of larger droplets.

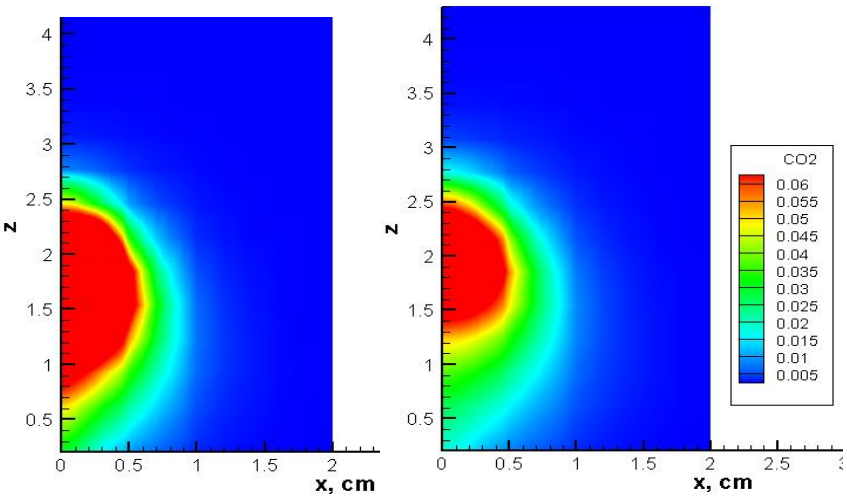

a) 2.5 ms b) 3ms

Fig. 9. CO_2 concentration fields during biodiesel combustion at a) t = 2.5 ms and b) t = 3 ms after the start of injection; Z (cm) –chamber's height projection; X (cm) – chamber's longitudinal projection

These larger droplets, having a greater size, are less prone to evaporation and fragmentation. Smaller droplets (5–15 μm), moving toward the chamber exit, evaporate more quickly and interact more actively with the airflow. This is also consistent with the Rosin-Rammler distribution, where such particles make up a larger proportion, enhancing the combustion process.

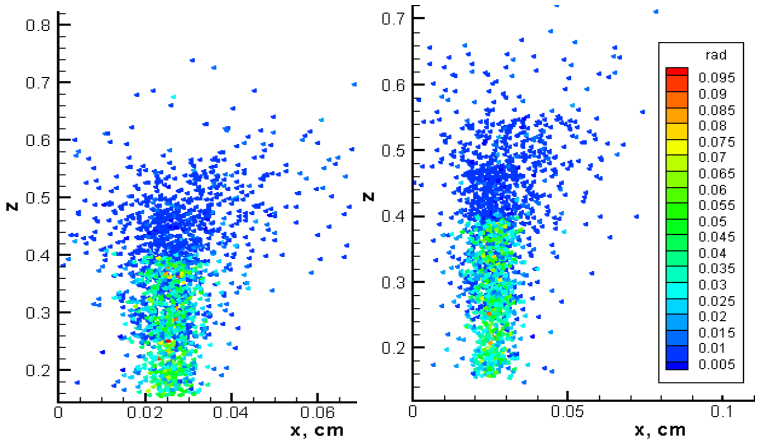

a) 2.5 ms b) 3ms

Fig. 10. Dispersion of biodiesel droplets by size at a) t = 2.5 ms and b) t = 3 ms after the start of injection: Z (cm) – chamber's height projection; X (cm) – chamber's longitudinal projection

Similarly, the evolution of the droplet sizes of heptane, a component of gasoline, shows a decrease in their maximum size from 10 μm to the range of 3–5 μm at the exit of the combustion chamber. This indicates more efficient droplet evaporation and their active interaction with the air flow, which likely contributes to improved combustion efficiency [32]. The highest oxygen consumption occurs at the center of the temperature flame, leading to the maximum fuel vapor concentration (0.28–0.32 g/g) along the axis of the combustion chamber at heights from 0.9 cm to 3.4 cm, as shown in Fig. 11.

This indicates more efficient combustion in this region. The fuel vapor concentration remains significantly lower in the rest of the chamber, ranging from 0.02 to 0.08 g/g. In other parts of the combustion chamber, the combustion process is less intense, which may lead to incomplete combustion and fuel wastage.

In the study of the aerodynamic characteristics of the reacting flow, a visualization of the longitudinal and transverse velocity components of biodiesel droplets was obtained at 2.5 ms and 3 ms after the start of injection (Fig. 12). A particle trajectory model was used to track the droplets, which allowed the measurement of droplet velocities of different sizes in various directions within the combustion chamber.

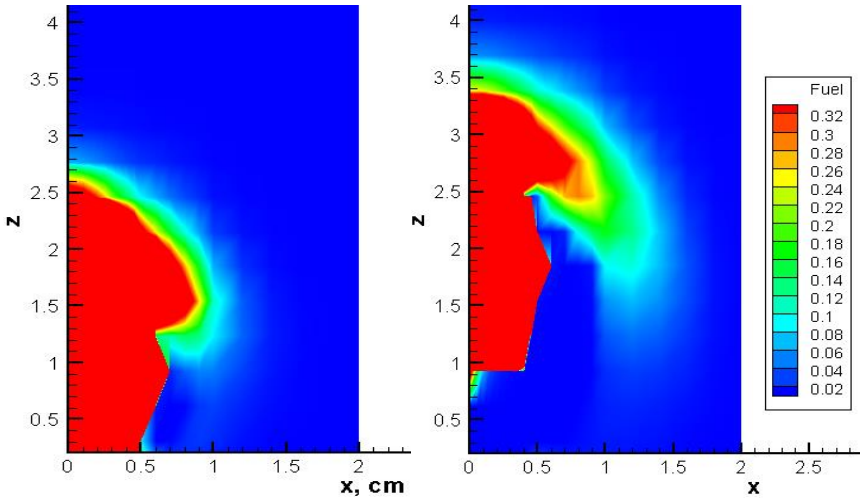

a) 2.5 ms b) 3ms

Fig. 11. Fuel vapor concentration fields during biodiesel combustion at a) t = 2.5 ms and b) t = 3 ms after the start of injection: Z (cm) – chamber's height projection; X (cm) – chamber's longitudinal projection

When burning traditional diesel fuel, a similar distribution of vapor concentration is observed. The maximum concentration of diesel vapor is recorded at a height of 3.8 cm of the combustion chamber, and in the rest of the combustion zone it is minimal, which indicates complete combustion of diesel fuel. For 4 ms, the minimum concentration of dodecane vapor is 0.01 g/g [33].

The maximum longitudinal velocity of the droplets at the outlet of the injector nozzle in the lower part of the chamber reached 24-36 m/s, and in the rest of the chamber and at the outlet it decreased to 4-10 m/s (Fig. 12a). In the cross-sectional plane of the chamber, the droplet velocity ranged from 3 to 5 m/s, as shown in Fig. 12b.

During gasoline's combustion, the following picture is observed. Droplets of gasoline are injected into a chamber with stationary gas, after which they are carried away by it and acquire a certain speed. During combustion, the highest speed of the drops is observed in the middle of the chamber, at about 1 cm from the center, where the optimal speed is from 1 to 3 m/s, which is significantly less than that of biofuel droplets [34].

This indicates that in the lower part of the combustion chamber, droplets move at higher speeds, improving their atomization and interaction with the air, which contributes to complete combustion. In the upper part of the chamber, droplets interact with the air less effectively due to their lower speed, which may reduce combustion efficiency. In the

chamber's cross-sectional plane, the droplet velocities distribution contributes to more uniform combustion.

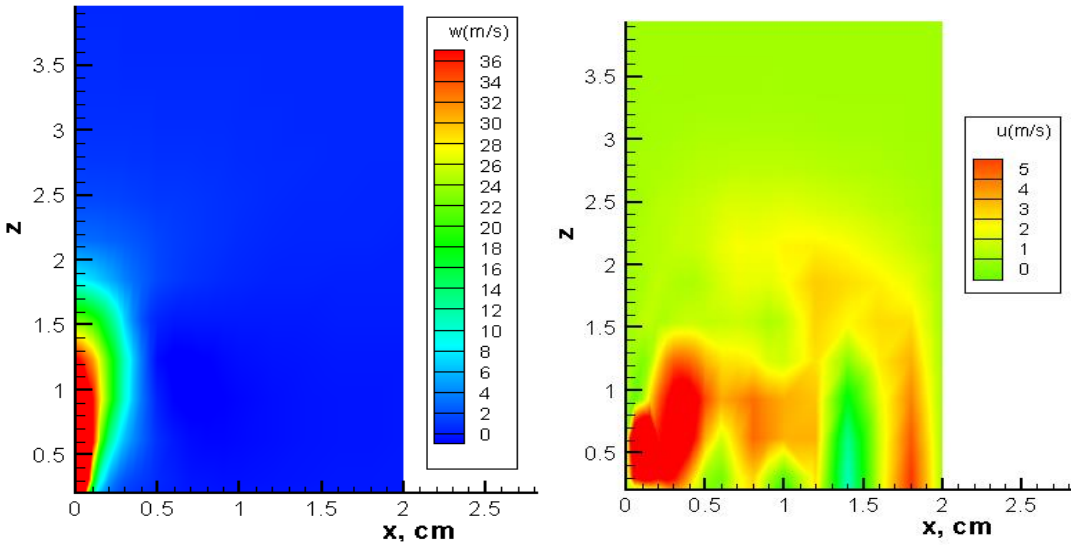

a) b)

Fig. 12. Aerodynamic characteristics of biodiesel droplets at 3 ms after the start of injection: *Z* (cm) – chamber's height projection; *X* (cm) – chamber's longitudinal projection, a) longitudinal velocity profile, b) cross-velocity profile

4. CONCLUSION

This paper provides a comprehensive analysis of biodiesel droplet atomization, combustion, and evaporation in an internal combustion engine using advanced computer models. It explores key factors affecting combustion efficiency and emissions, along with a comparative evaluation against traditional diesel fuel.

1. Modeling has shown that biodiesel achieves higher combustion temperatures than conventional diesel fuel. The maximum combustion temperature of biodiesel reaches 2700 K, while for diesel fuel the maximum temperature is 1800 K. This is due to the high calorific value and chemical composition of biodiesel, which promotes more complete combustion and lower emissions of carbon dioxide (CO_2) and carbon monoxide (CO);

2. Carbon monoxide (CO) emissions decrease for both biodiesel and diesel fuel as injection temperatures increase. Biodiesel exhibits lower CO levels than conventional diesel fuel, especially at high injection temperatures without considering hydrocarbon dissociation and ion-based chemical reactions. This is due to the better oxidizability of biodiesel due to the high oxygen content in its molecules;

2. Modelling of biodiesel atomization has shown that droplet diameters decrease with increasing injection temperature, which improves evaporation and more complete combustion. Small droplets evaporate faster and their interaction with air is enhanced, which improves combustion efficiency and reduces emissions of pollutants such as carbon monoxide and soot;

3. The pressure in the combustion chamber significantly affects soot emissions. Soot emissions are significantly reduced when the pressure increases to 40 bar due to the improved

combustion process. Increasing the pressure increases the temperature and turbulence, which leads to more complete combustion of the fuel;

4. Visualization of the aerodynamic characteristics of droplets showed that biodiesel droplets in the lower part of the combustion chamber move at high speed (20–24 m/s), which contributes to their better atomization and mixing with air. This improves the combustion process and increases the efficiency of biofuel use;

5. Ultimately, the study demonstrates that biodiesel is an effective alternative to traditional hydrocarbon fuels, offering reduced carbon oxides and soot emissions while enhancing combustion efficiency through smaller droplet sizes and more complete evaporation.

FUNDING

This work was supported by the Science Committee of the Ministry of Science and Higher Education of the Republic of Kazakhstan (grant number AP19679741).

REFERENCES

[1] International Energy Agency (IEA) report. Biofuels. Available at: https://www.iea.org/energy-system/low-emission-fuels/biofuels.

[2] International Energy Agency (IEA) report. Transport biofuels. Available at: https://www.iea.org/reports/renewables-2023/transport-biofuels.

[3] ASKAROVA A., BOLEGENOVA S., OSPANOVA S., BOLEGENOVA S., BAIDULLAYEVA G., BERDIKHAN K., NUSSIPZHAN A., 2024, *Determining the Optimal Oxidation Temperature of Non-Isothermal Liquid Fuels Injections Using Modelling Based on Statistical Droplet Distribution*, East-Eur J. Enterp. Technol., 6/8, 132, 44–55.

[4] ZHONG W., MAHMOUD N.M., WANG Q., 2022, *Numerical Study of Spray Combustion and Soot Emission of Gasoline-Biodiesel Fuel under Gasoline Compression Ignition-Relevant Conditions*, Fuel, 310/A, 122293.

[5] ZANDIE M., NG H.K., GAN S., MUHAMAD SAID M.F., CHENG X., 2022, *Development of a Reduced Multi-Component Chemical Kinetic Mechanism for the Combustion Modelling of Diesel-Biodiesel-Gasoline Mixtures*, Transp. Eng., 7, 100101.

[6] NEMA V.K., SINGH A., CHAURASIYA P.K., GOGOI T.K., VERMA T.N., TIWARI D., 2023, *Combustion, Performance, and Emission Behaviour of a CI Engine Fuelled with Different Biodiesels: A Modelling, Forecasting and Experimental Study*, Fuel, 339, 126976.

[7] KRISHNASAMY A., BUKKARAPU K.R., 2021, *A Comprehensive Review of Biodiesel Property Prediction Models for Combustion Modelling Studies*, Fuel, 121085.

[8] UYUMAZ A., 2020, *Experimental Evaluation of Linseed Oil Biodiesel/Diesel Fuel Blends on Combustion, Performance and Emission Characteristics in a DI Diesel Engine*, Fuel, 267, 117150.

[9] ZHAO J., WANG J., 2013, *Control-Oriented Multi-Phase Combustion Model for Biodiesel Fueled Engines*, Appl. Energy, 108, 92–99.

[10] CAI G., YEN M., ABRAHAM J., 2016, *On Formulating a Simplified Soot Model for Diesel and Biodiesel Combustion*, Chem. Eng. Sci., 144, 249–259.

[11] CAN Ö., ÖZTÜRK E., SERDAR YÜCESU H., 2017, *Combustion and Exhaust Emissions of Canola Biodiesel Blends in a Single Cylinder DI Diesel Engine*, Renew Energy, 109, 73–82.

[12] ANANTHA RAMAN L., DEEPANRAJ B., RAJAKUMAR S., SIVASUBRAMANIAN V., 2019, *Experimental Investigation on Performance, Combustion and Emission Analysis of a Direct Injection Diesel Engine Fuelled with Rapeseed Oil Biodiesel*, Fuel, 246, 69–74.

[13] ALDHAIDHAWI M., CHIRIAC R., BADESCU V., 2017, *Ignition Delay, Combustion and Emission Characteristics of Diesel Engine Fuelled with Rapeseed Biodiesel – A Literature Review*, Renew Sustain Energy Rev., 73, 178–186.

[14] ASKAROVA A., BOLEGENOVA S., OSPANOVA SH., RAKHIMZHANOVA L., NURMUKHANOVA A., ADILBAYEV N., 2024, *Optimization of Fuel Droplet Sputtering and Combustion at High Turbulence Flows*, Russ. Phys J, 67, 167–170.
[15] BOLEGENOVA S., ASKAROVA A., OSPANOVA SH., MAKANOVA A., ZHUMAGALIYEVA S., NURMUKHANOVA A., ADILBAYEV N., AKZHOL SH. *Simulation of Liquid Fuel Spray Formation and Distribution in a Reacting Turbulent Flow*, Eurasian Phys. Tech. J., 21, 22–30.
[16] LAUNDER B.E., SPALDING D.B., 1974, *The Numerical Computation of Turbulent Flows*, Comput. Methods Appl. Mech. Eng., 3, 269–289.
[17] LEITHNER R., MAXIMOV V., ERGALIEVA A., et al, 2016, *Computational Modelling of Heat and Mass Transfer Processes in Combustion Chamber at Power Plant of Kazakhstan*, MATEC Web Conf., 76, 06001.
[18] AARNE VESILIND P., 1980, *The Rosin-Rammler Particle Size Distribution*, Resour. Conserv. Recycl., 5, 275–277.
[19] DOMINGO-ALVAREZ P., BENARD P., MOUREAU V., et al, 2020, *Impact of Spray Droplet Distribution on the Performances of a Kerosene Lean/Premixed Injector*, Flow Turbulence Combust, 104, 421–450.
[20] DUKE-WALKER V., MUSICK B.J., MCFARLAND J.A., 2023, *Experiments on the Breakup and Evaporation of Small Droplets at High Weber Number*, Int. J. Multiph. Flow, 161, 104389.
[21] SHAO CH., LUO K., YANG Y., FAN J., 2018, *Direct Numerical Simulation of Droplet Breakup in Homogeneous Isotropic Turbulence: The Effect of the Weber Number*, Int. J. Multiph. Flow, 107, 263–274.
[22] PILCH M., ERDMAN C.A., 1987, *Use of Breakup Time Data and Velocity History Data to Predict the Maximum Size of Stable Fragments for Acceleration-Induced Breakup of a Liquid Drop*, Int. J. Multiph. Flow, 13, 741–757.
[23] MACPHERSON G.B., NORDIN N., WELLER H.G., 2009, *Particle Tracking in Unstructured, Arbitrary Polyhedral Meshes for Use in CFD and Molecular Dynamics*, Commun. Numer. Meth. En., 25, 263–273.
[24] KULESHOV A., MAHKAMOV K., 2008, *Multi-Zone Diesel Fuel Spray Combustion Model for the Simulation of a Diesel Engine Running on Biofuel*, Proc. Inst. Mech. Eng., A, 222, 309–321.
[25] KULESHOV A., 2007, *Multi-Zone DI Diesel Spray Combustion Model and its Application for Matching the Injector Design with Piston Bowl Shape*, SAE Tech. Pap., 2007–01–1908.
[26] AMSDEN A.A., O'ROURKE P.J., BUTLER T.D., 1980, KIVA-II: *A Computer Program for Chemically Reactive Flows with Sprays*, Los Alamos, 160.
[27] RODRIGUEZ R.P., SIERENS R., VERHELST S., 2011, *Ignition Delay in a Palm Oil and Rapeseed Oil Biodiesel Fuelled Engine and Predictive Correlations for the Ignition Delay Period*, Fuel, 90, 766–772.
[28] GOROKHOVSKI M., BORGHI R., 1993, *Numerical Simulation of Soot Formation and Oxidation in Diesel Engines*, SAE Trans., 102, 118–130.
[29] TAO F., GOLOVITCHEV V.I., CHOMIAK J., 2004, *A Phenomenological Model for the Prediction of Soot Formation in Diesel Spray Combustion*, Combust Flame 136, 270–282.
[30] LESNIK L., BILUS I., 2016, *The Effect of Rapeseed Oil Biodiesel Fuel on Combustion, Performance, and the Emission Formation Process within a Heavy-Duty DI Diesel Engine*, Energy Convers Manage, 109, 140–152.
[31] ASKAROVA A., BOLEGENOVA S., MAZHRENOVA N., et al, 2016, *3D Modelling of Heat and Mass Transfer Processes During the Combustion of Liquid Fuel*, Bulg. Chem. Commun., 28, 229–235.
[32] BOLEGENOVA S., ASKAROVA A., SLAVINSKAYA N., OSPANOVA SH., MAXUTKHANOVA A., ALDIYAROVA A., YERBOSYNOV D., 2022, *Statistical Modelling of Spray Formation, Combustion, and Evaporation of Liquid Fuel Droplets*, Phys. Sci. Technol., 9, 69–82.
[33] ASKAROVA A., BOLEGENOVA S., OSPANOVA SH., SLAVINSKAYA N., ALDIYAROVA A., UNGAROVA N., 2021, *Simulation of Non-Isothermal Liquid Sprays Under Large-Scale Turbulence*, Phys. Sci. Technol., 8, 28–40.
[34] BOLEGENOVA S., ASKAROVA A., OSPANOVA S., ZHUMAGALIYEVA S., MAKANOVA A., ALDIYAROVA A., NURMUKHANOVA A., IDRISSOVA G., 2024, *Technology of Reducing Greenhouse Gas Emissions for Decarbonization and Decreasing Anthropogenic Pressure on the Environment*, Phys. Sci. Technol., 11, 64–75.